Effect of Styryl Side Groups on the Photophysical Properties and Hole Mobility of PPE−PPV Systems

Daniel A. M. Egbe,*,†,‡ Emine Tekin,† Eckhard Birckner,§ Almantas Pivrikas,|| Niyazi S. Sariciftci,|| and Ulrich S. Schubert*,†,‡

Laboratory of Macromolecular Chemistry and Nanoscience, Eindhoven University of Technology and Dutch Polymer Institute (DPI), P.O. Box 513, 5600 MB Eindhoven, The Netherlands, Laboratory for Organic and Macromolecular Chemistry, Friedrich-Schiller-University Jena, Humboldtstrasse 10, D-07743 Jena, Germany, Institute of Physical Chemistry, Friedrich-Schiller-University Jena, Lessingstrasse 10, D-07743 Jena, Germany, and Linz Institute of Organic Solar Cells (LIOS), Department of Physical Chemistry, Johannes Kepler University, Altenbergerstrasse 69, A-4040 Linz, Austria

Received July 27, 2007; Revised Manuscript Received August 15, 2007

ABSTRACT: This contribution reports on the synthesis of defect-free styryl-substituted poly(*p*-phenylene−ethynylene)-*alt*-poly(*p*-phenylene−vinylene)s, **DO-** and **MEH-ST-PPE$_2$-PPV$_2$**, consisting of a 2:2 *triple bond*/*double bond* ratio in the main chain. A detailed and systematic comparison of their photophysical properties with those of solely alkoxy-substituted polymer **O-8-PPE$_2$-PPV$_2$**, highlighting the effect of the styryl side groups, has been carried out. The bis(styryl) substituents act on the one hand as electron donor to the main chain conjugation system and, on the other hand, form a separate bis(styryl)phenylene chromophore system. The resulting two-dimensional and separate conjugation construct in **ST-PPE-PPV** polymers is confirmed by the fluorescence excitation anisotropy curves, which reach the value 0 around 360 nm corresponding to the absorption of the bis(styryl) system. Thin film PL and EL spectra of **MEH-ST-PPE$_2$-PPV$_2$** are red-shifted relative to **DO-ST-PPE$_2$-PPV$_2$**, due to strong $\pi-\pi$ interchain interactions resulting from the grafting of methoxy side groups, potentially explaining the better EL performance of **MEH-** than **DO-ST-PPE$_2$-PPV$_2$** LED device (glass substrate/ITO/PEDOT:PSS/**ST-PPE$_2$-PPV$_2$**/Ca/Ag) as well as the higher intrinsic hole mobility value, μ_{hole} (measured using CELIV technique) for **MEH-** (2.8×10^{-6} cm^2/V·s) than **DO-ST-PPE$_2$-PPV$_2$** (1.5×10^{-6} cm^2/V·s). Both values are, however, at least 2-fold lower than that of **O-8-PPE$_2$-PPV$_2$** (5.5×10^{-6} cm^2/V·s) due to the twist in their conjugated backbone caused by the styryl side groups. Nevertheless, nonoptimized bulk heterojunction solar cells of $\eta_{AM1.5}$ around 1% were readily designed using **MEH-ST-PPE$_2$-PPV$_2$** as donor and PCBM as acceptor in a 1:3 weight ratio.

Introduction

Poly(-*p*-phenylene-ethynylene)-*alt*-poly(-*p*-phenylene-vinylene)s (PPE-PPVs) are a class of conjugated systems combining the interesting intrinsic properties of both poly(-*p*-phenylene-ethynylene)s (PPEs) and poly(-*p*-phenylene-vinylene)s (PPVs) into a single polymeric backbone, resulting in additional structure-specific properties.[1−4] They have found so far applications in light-emitting diodes,[4a,5−6] in nonlinear optics,[7] and in organic solar cells,[3a] where they have been used either as donor[8−9] or acceptor[5d,10] components.

The properties of PPE-PPV systems consisting of a 2:2 ratio of *triple bond*/*double bond* and of the general constitutional unit: $(Ph-C\equiv C-Ph-C\equiv C-Ph-CH=CH-Ph-CH=CH-)_n$ are known to show a strong dependence on the *number*, *position*, and *nature* of the grafted alkoxy side chains. For instance, increasing the number of alkoxy side chains from **4-PPE$_2$-PPV$_2$** to **8-PPE$_2$-PPV$_2$** in the repeating unit leads to a bathochromic shift of 20 nm of the absorption maximum (from 450 to 470 nm) and 30 nm of the emission maximum (from 490 to 520 nm) in dilute chloroform solution (Figure 1).[2b]

In this contribution, we investigate the effect of replacing both alkoxy side groups at R^2 in **8-PPE$_2$-PPV$_2$** with styryl units; this results in polymers denoted **ST-PPE$_2$-PPV$_2$**, which can be considered as two-dimensional conjugated systems due to the insaturation of the styryl units.

To the best of our knowledge very few examples of conjugated polymers bearing bis(styryl) side groups are known in the literature. Bunz et al. made the first report on PPE systems decorated with various bis(styryl) units.[11] This was followed by a report by Egbe et al. on a bis(styryl)-containing PPE-PPV polymer, **ST-PPE$_2$-PPV$_1$** (Figure 2), whose main chain consisted of a 2:1 *triple bond*/*double bond* ratio.[5a] In both cases the photophysical investigations were limited on the absorption and emission spectra and fluorescence quantum yields, in order to elucidate the effect of the unsaturated side groups. In this work, in contrast, a more extensive and detailed approach (absorption spectra, absorption coefficients, emission spectra, fluorescence quantum yields, fluorescence anisotropy as well as fluorescence lifetimes and rate constants) was taken, which better highlights the effect of the styryl side groups on the photophysical properties of **DO-ST-PPE$_2$-PPV$_2$** and **MEH-ST-PPE$_2$-PPV$_2$** and their luminophoric starting materials **7** and **8** (Scheme 1). These studies took into consideration the solely alkoxy-substituted congener **O-8-PPE$_2$-PPV$_2$** with its monomer **10** as well as **ST-PPE$_2$-PPV$_1$** for purpose of comparison.

* To whom correspondence should be addressed. E-mail: (D.A.M.E.) c5ayda@uni-jena.de; (U.S.S.) U.S.Schubert@tue.nl.

† Laboratory of Macromolecular Chemistry and Nanoscience, Eindhoven University of Technology and Dutch Polymer Institute (DPI).

‡ Laboratory for Organic and Macromolecular Chemistry, Friedrich-Schiller-University Jena.

§ Institute of Physical Chemistry, Friedrich-Schiller-University Jena.

|| Linz Institute of Organic Solar Cells (LIOS), Department of Physical Chemistry, Johannes Kepler University.

10.1021/ma071676i CCC: $37.00
Published on Web 10/04/2007

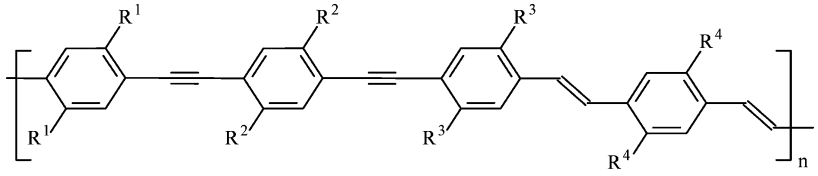

4-PPE$_2$-PPV$_2$: $R^1 = R^3 = H$, $R^2 = R^4 =$ alkoxy
8-PPE$_2$-PPV$_2$: $R^1 = R^2 = R^3 = R^4 =$ alkoxy
ST-PPE$_2$-PPV$_2$: $R^1 = R^3 = R^4 =$ alkoxy, $R^2 =$ styryl

Figure 1. General schematic structures of polymers denoted **4-PPE$_2$-PPV$_2$**, **8-PPE$_2$-PPV$_2$**, and **ST-PPE$_2$-PPV$_2$**.

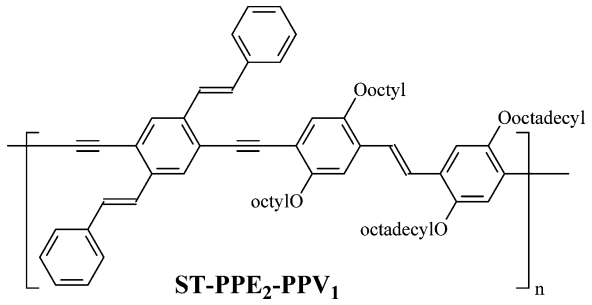

ST-PPE$_2$-PPV$_1$

Figure 2. Chemical structure of **ST-PPE$_2$-PPV$_1$**.

Intrinsic hole mobilities of the three **PPE$_2$-PPV$_2$** polymers have been measured using charge carrier extraction by linearly increasing voltage (CELIV) technique. Preliminary photovoltaic studies were subsequently performed on **MEH-ST-PPE$_2$-PPV$_2$**, exhibiting an approximately twice higher μ_{hole} value than **DO-ST-PPE$_2$-PPV$_2$**.

Experimental Part

Instrumentation. ^{1}H NMR and ^{13}C NMR spectra were obtained in deuterated chloroform using either a Bruker DRX 400 or a Bruker AC 250. Chemical shifts (δ values) are given in parts per million with tetramethylsilane as an internal standard. Elemental analyses were measured on a CHNS-932 Automat Leco or a Euro Vector EuroEA3000 elemental analyzer for CHNS. Infrared spectroscopy was recorded on a Nicolet Impact 400. Gel-permeation chromatography (GPC) was performed on a set of Knauer or on a Shimadzu system using THF as eluent and polystyrene as a standard. Thermogravimetric analyses were performed in a TG 209 F1 Iris by Netzsch under a nitrogen atmosphere in the range from 30 to 500 °C with a heating rate of 20 °C/min. The absorption spectra were recorded in dilute chloroform or THF solution on a Perkin-Elmer UV/vis-NIR spectrometer Lambda 19. Fluorescence spectra were measured in dilute chloroform solution with a LS 50B luminescence spectrometer (Perkin-Elmer). The relative photoluminescence quantum yields in solution were calculated from the quantum-corrected spectra according to Demas and Crosby against quinine sulfate in 0.1 N sulfuric acid as a standard ($\Phi_f = 55\%$).[12] The anisotropy spectra were calculated from the fluorescence excitation spectra measured with the parallel and perpendicular orientated polarizer and analyzer. The fluorescence lifetimes are determined from the fluorescence decay curves measured with a CD900 time correlating single photon counting spectrometer (Edinburgh Instruments). The films were spin-casted from chlorobenzene solution. The quantum yield in solid-state was determined against a CF_3P−PPV (poly{1,4-phenylene-[1-(4-trifluoromethylphenyl)vinylene]-2,5-dimethoxy-1,4-phenylene-[2-(4-trifluoromethylphenyl)vinylene]}) copolymer reference whose quantum yield has been measured by integrating sphere to be 0.43.[2]

Mobility Measurements. Sandwich-type samples were used in the transport measurements, where the bulk charge carrier mobility was measured in thick polymer films. The polymers were dissolved in chlorobenzene with a concentration of 10 mg/mL. The solutions were filtered through a 0.45 μm filter before deposition by drop casting on top of pre-patterned ITO-covered glass substrates. Finally, 100 nm aluminum top electrodes with typical dimensions of 2−8 mm^2 were evaporated on top of the polymer in vacuum under 10^{-6} mbar. The samples were prepared in normal atmosphere and the films were measured in the nitrogen cryostat (Oxford Optistat DNV) under vacuum. For CELIV experiment a variable pulse generator (Agilent 33250A) and the oscilloscope (Tektronix TDS 754C) were used to record the extraction current transients. For triggering purposes to ensure the proper delay time between voltage and light pulse, a pulse and delay function generator (Stanford DG535) was used. Nd:YAG laser (Coherent Infinity 40−100) was utilized for the charge carriers photoexcitations, with a light pulse width of 5 ns, wavelength 355 nm with energy of less than 1 mJ per pulse. The thick films (1−5 μm) were illuminated through the ITO side, therefore giving a possibility to prove for both electron and hole mobilities under different applied biases.

Electroluminescent Studies. The LED device (configuration: glass substrate/ITO/PEDOT:PSS/**ST-PPE$_2$-PPV$_2$**/Ca/Ag) characterization was done with a Keithley 2400 source meter, a calibrated photodiode and an Ocean Optics SD2000 CCD spectrometer under argon atmosphere.

Solar Cell Studies. Solar cell fabrication and parameters measurement were carried out under similar experimental conditions as described elsewhere.[15]

Materials. All starting materials were purchased from commercial suppliers (Fluka, Merck, and Aldrich). Toluene was dried and distilled over sodium and benzophenone. Diisopropylamine was dried over KOH. If not otherwise specified solvents or solution were degassed by bubbling with argon or nitrogen 1 h prior to use.

***trans,trans*-2,5-Distyryl-1,4-dibromobenzene (5)** was obtained in a four-step reaction starting from xylol as described in the literature and as shown in Scheme 1.[13] The syntheses of 4-ethynyl-2,5-dioctyloxybenzaldehyde (**6**)[5b,14] and 2,5-bis(alkoxy)-*p*-xylylene-bis(diethylphosphonate) (**9**)[15] have been described elsewhere.

***trans,trans*-2,5-Distyryl-1,4-bis(4-formyl-2,5-dioctyloxyphenylethynyl)benzene (7) and *trans,trans*-2,5-Distyryl-4-bromo-1-(4-formyl-2,5-dioctyloxyphenylethynyl)benzene (8).** *trans,trans*-2,5-Distyryl-1,4-dibromobenzene (**5**) (2 g, 4.54 mmol), 4-ethynyl-2,5-dioctyloxybenzene (4 g, 10.34 mmol), $Pd(PPh_3)_4$ (209 mg, 1.816×10^{-4} mol, 4 mol %), and CuI (34 mg, 1.816×10^{-4} mol, 4 mol %) were given to a degassed solution of 30 mL of diisopropylamine and 80 mL of toluene. The reaction mixture was heated at 70−80 °C for 24 h in an argon atmosphere. After the reaction was cooled to room temperature, the precipitated diisopropylammonium bromide was filtered off and the solvent removed under vacuum. The residue was chromatographed on a silica gel column using a mixture of toluene/hexane (10/1) as eluent. 1.90 g (40%, $R_f = 0.48$) of the desired product **7** was obtained as yellow powder alongside 1.12 g (33%, $R_f = 0.70$) of monobrominated compound **8**.

7. ^{1}H NMR (400 MHz, $CDCl_3$): δ/ppm 0.77−1.84 (60H, CH_3-$(CH_2)_6$−), 3.92−4.07 (8H, −CH_2O−), 7.11−7.92 (20H, phenylene and vinylene H's), 10.46 (2H, −CHO). ^{13}C NMR (100 MHz, $CDCl_3$): δ/ppm 13.97, 14.01 (CH_3−), 22.54, 22.60, 25.85, 26.04, 28.98, 29.14, 29.16, 29.17, 29.20, 29.26, 31.70, 31.75 (−$(CH_2)_6$−), 69.33, 69.62 (−CH_2O−), 91.98, 95.39 (−C≡C−), 110.30, 117.42, 120.24, 122.47, 125.22, 125.25, 125.64, 126.91, 128.09, 128.17, 128.66, 128.96, 128.98, 131.05, 137.21, 137.66, 137.80 (phenylene and vinylene C's), 153.82, 155.49 (C_{phenyl}−OR), 189.00 (−CHO). FTIR: 3060 (w, C_{phenyl}−H), 2922 and 2854 (s, CH_3 and

Scheme 1

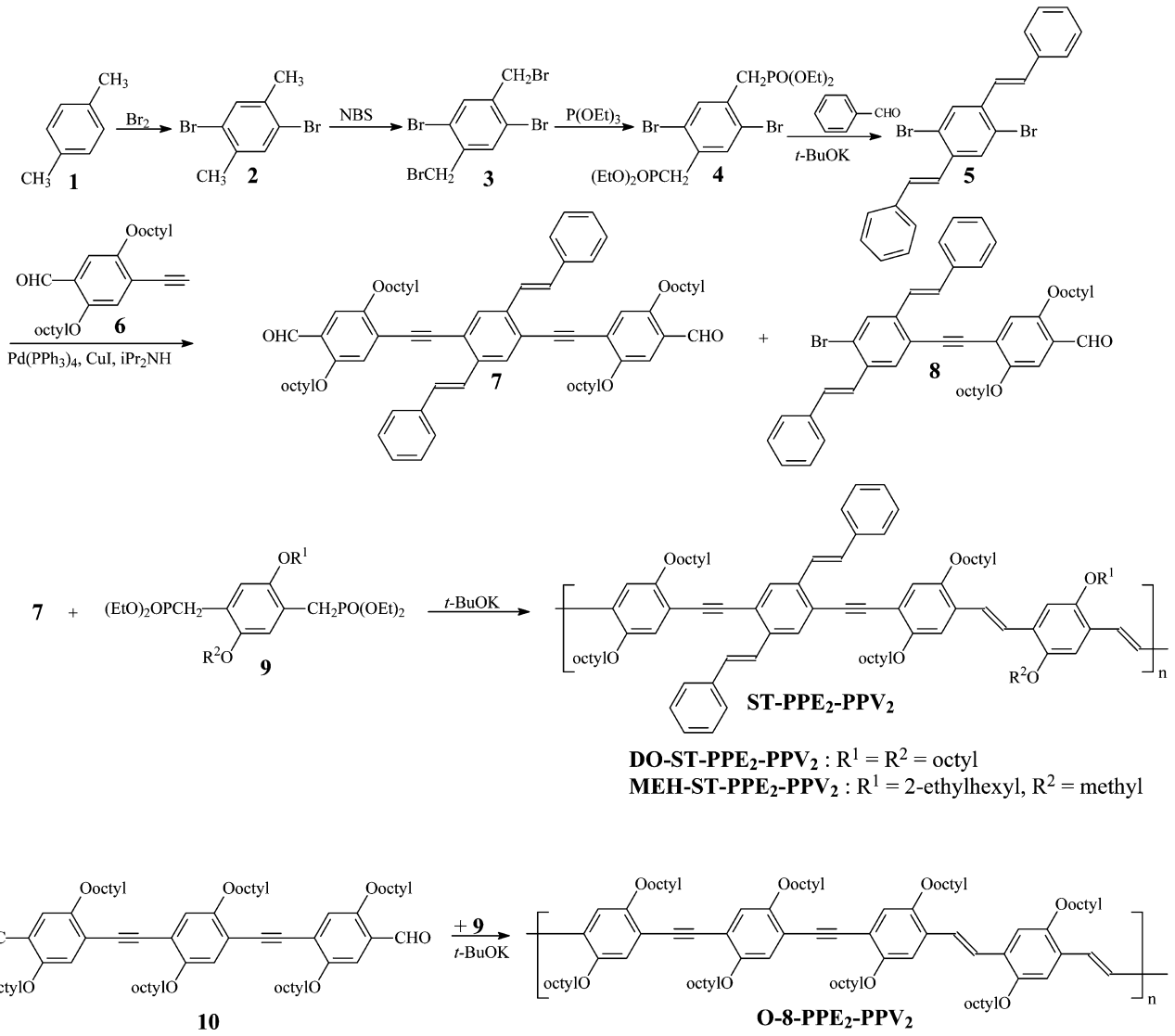

−CH_2−), 1666 (s, −CHO), 1602 (s, C═C_{phenyl}), 1388 (s, CH_3), 1211 (C_{phenyl}-OR), 970 (s, trans −CH═CH−), 738 and 693 (s, monosubstituted benzene). UV−vis ($CHCl_3$) (λ_{max} (ϵ in L·mol^{-1}·cm^{-1})): 340.4 (77 600), 370 (67600). Anal. Calcd for $C_{72}H_{88}O_6$ (1049.48): C, 82.40; H, 8.45. Found: C, 82.19; H, 8.56.

8. ^{1}H NMR (250 MHz, $CDCl_3$): δ/ppm 0.69−1.77 (30H, CH_3-$(CH_2)_6$-), 3.94−4.00 (4H, t,^3J = 6.55 Hz, −CH_2O−), 7.04−7.87 (18H, phenylene and vinylene H's), 10.39 (1H, s, −CHO). ^{13}C NMR (63 MHz, $CDCl_3$): δ/ppm 14.07, 14.12 (CH_3−), 22.61, 22.68, 25.89, 26.09, 28.99, 29.21, 29.24, 29.33, 31.75, 31.81 (−$(CH_2)_6$−), 69.27, 69.57 (−CH_2O−), 91.17, 94.80 (−C≡C−), 110.17, 117.31, 120.19, 121.37, 124.99, 125.09, 126.30, 126.92, 127.04, 128.29, 128.72, 128.81, 129.15, 130.24, 131.46, 131.87, 134.17, 134.39, 135.96, 136.81, 136.98, 139.17 (phenylene and vinylene C's), 153.73, 155.51 (C_{phenyl}−OR), 189.14 (CHO).

FTIR: 3056 (w, C_{phenyl}−H), 2922 and 2851 (s, CH_3 and −CH_2−), 1677 (s, −CHO), 1603 (s, C═C_{phenyl}), 1386 (s, CH_3), 1208 (C_{phenyl}−OR), 960 (s, trans −CH═CH−), 747 and 688 (s, monosubstituted benzene). UV−vis ($CHCl_3$) (λ_{max} (ϵ in L·mol^{-1}·cm^{-1})): 332.0 (55 300), 363.2 (55 000). Anal. Calcd for $C_{47}H_{53}O_4$-Br (745.84): C, 75.69; H, 7.16; Br, 10.71 Found: C, 73.57; H, 7.08; Br, 10.97.

Poly[1,4-(2,5-dioctyloxy)phenylene-ethynylene-1,4-(2,5-distyryl)-phenylene-ethynylene-1,4-(2,5-dioctyloxy)phenylene-vinylene-1,4-(2,5-dioctyloxy)phenylene-vinylene] (DO-ST-PPE$_2$-PPV$_2$). Bis(styryl)-containing dialdehyde **7** (200 mg, 1.9 × 10^{-4} mol) and 2,5-dioctyloxy-*p*-xylylenebis(diethylphosphonate) (121 mg, 1.9 × 10^{-4} mol) were dissolved in toluene (20 mL) with vigorous stirring under argon and heating under reflux. Potassium *tert*-butoxide (130 mg) was added in portions to this solution; and the reaction mixture was heated at reflux for 2 h and 15 min before adding 50 μL of benzaldehyde. After a total reaction time 2 h 45 min more toluene (30 mL) was added and the reaction was quenched with 10% aqueous HCl solution (20 mL). The organic phase was separated and extracted several times with distilled water until the water phase became neutral (pH = 6−7). The organic layer was dried with a Dean−Stark apparatus. The resulting toluene suspension was filtered and evaporated under reduced pressure to 20 mL and was precipitated in 400 mL of methanol. After extraction in diethyl ether and drying under vacuum, 152 mg of a dark red substance was obtained. Yield: 58%. GPC (THF): M_w = 46 600 g/mol, M_n = 14 200 g/mol, polydispersity index (PDI) = 3.23. ^{1}H NMR (300 MHz, CD_2Cl_2): δ/ppm 0.86−1.95 (octyl H's); 3.75−4.15 (C**H**$_2$O); 6.84−8.01 (phenylene and vinylene H's). ^{13}C NMR (75 MHz, $CDCl_3$): δ/ppm 13.63 (**C**H$_3$), 22.26, 25.70, 25.87, 25.95, 28.86, 29.06, 29.24, 31.42, 31.50 (−CH_2−), 69.26, 69.32, 69.84 (**C**H$_2$O); 92.67 (−**C**≡**C**−); 110.70, 110.87, 112.43, 116.87, 122.39, 123.05, 124.52, 126.59, 127.46, 128.26, 128.42, 129.01, 137.03, 137.26 (phenylene and vinylene C's); 150.36, 151.00, 154.08 (**C**$_{aryl}$−OR). FTIR (KBr): 3062 (w, ν_{CH}); 2923 (s, ν_{as} CH_2), 2854 (m, ν_s CH_2), 2200 (w, $\nu_{C\equiv C}$), 1597 (m, $\nu_{C=C}$); 1202 (vs, $\nu_{C_{aryl}-OR}$), 961 (s, $\nu_{CH=CH}$ trans) cm^{-1}. UV−vis ($CHCl_3$) (λ_{max} (ϵ in L·mol^{-1}·cm^{-1})): 340 (44 600), 366 (47 200), 467.5 (75 700). Anal. Calcd for $(C_{96}H_{128}O_6)_n$ $(1378.06)_n$: C, 83.67; H, 9.36. Found: C, 82.28; H, 9.63.

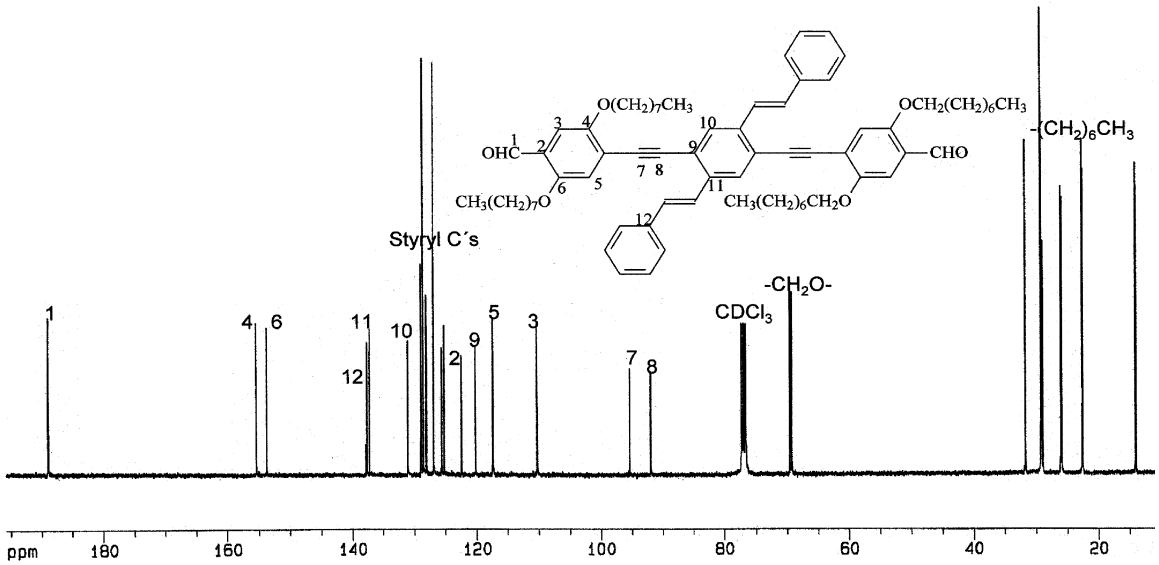

Figure 3. ^{13}C NMR spectrum (100 MHz, $CDCl_3$) of dialdehyde **7**.

Poly[1,4-(2,5-dioctyloxy)phenylene—ethynylene-1,4-(2,5-distyryl)phenylene-ethynylene-1,4-(2,5-dioctyloxy)phenylene-vinylene-1,4-[2-(2-ethyl)hexyloxy-5-methoxy]phenylene-vinylene] (MEH-ST-PPE$_2$-PPV$_2$). Bis(styryl)-containing dialdehyde **7** (500 mg, 0.475 mmol) and 2-(2′-ethylhexyloxy)-5-methoxy-*p*-xylylene-*bis*-(diethylphosphonate) (255 mg, 0.475 mmol) were dissolved in toluene (20 mL) while stirring vigorously under argon and heating under reflux. Potassium *tert*-butoxide (158 mg, 1.4 mmol) was added in portions to this solution, and the reaction mixture was heated at reflux for 3 h. After this time, more toluene was added, and the reaction was quenched with 10% aqueous HCl solution (20 mL). The organic phase was separated and extracted several times with distilled water until the water phase became neutral (pH = 6−7). The organic layer was dried with a Dean−Stark apparatus. The resulting toluene suspension was filtered and evaporated under reduced pressure to 30 mL and was precipitated in 300 mL methanol. After extraction with methanol, then with acetone, 480 mg of dark red substance were obtained. Yield: 96%. GPC (THF): M_w = 100 000 g/mol, M_n = 27 000 g/mol, M_z = 286 000 g/mol, polydispersity index (PDI) = 3.74. ^1H NMR (250 MHz, $CDCl_3$): δ/ppm 0.71−1.73 (octyl and 2-ethylhexyl H's), 3.42−4.04 (CH_3O− and −CH_2O−); 7.03−7.88 (phenylene and vinylene H's). ^{13}C NMR (63 MHz, $CDCl_3$): δ/ppm 11.35 (**C**H_3 ethyl), 14.08 (**C**H_3 hexyl), 22.65, 23.12, 24.27, 26.00, 26.19, 29.33, 30.87, 31.78 (**C**H_2), 39.74 (**C**H); 56.24 (O**C**H_3); 69.36, 69.76, 70.07, 71.65 (**C**H_2O), 92.91 (**C C**), 110.17, 111.00, 112.44, 116.93, 122.66, 126.93, 127.86, 128.62, 137.46 (phenylene and vinylene C's); 150.60, 151.38, 151.52, 154.30 (**C**$_{phenyl}$−OR). IR (KBr): 3065 (w, ν_{CH}); 2953 (m, $\nu_{as(CH_3)}$); 2923 (s, $\nu_{as(CH_2)}$); 2854 (m, $\nu_{s(CH_2)}$); 2202 (w, $\nu_{C\equiv C}$) 1596 (m, $\nu_{C=C}$); 1202 (vs, $\nu_{C_{aryl}-OR}$), 958 (s, $\nu_{CH=CH}$ trans) cm^{-1}. UV−vis ($CHCl_3$) (λ_{max} (ϵ in L·mol^{-1}·cm^{-1})): 339.6 (50 100), 470.8 (82 300). Anal. Calcd for $(C_{89}H_{114}O_6)_n$ (1279.88)$_n$: C, 83.52; H, 8.98. Found: C, 82.69; H, 9.11.

Results and Discussion

The synthetic path to **ST-PPE$_2$-PPV$_2$**, as illustrated in Scheme 1, requires the preliminary synthesis of distyryl-containing dialdehyde **7**. Compound **7** is a product from the Pd-catalyzed Sonogashira cross-coupling reaction[16] of *trans*,*trans*-2,5-distyryl-1,4-dibromobenzene (**5**) (obtained in a four-step reaction starting from *p*-xylol)[13] with 4-ethynyl-2,5-dioctyloxybenzaldehyde (**6**).[5b,14] It was obtained as a yellow powder in 40% yield alongside the monobrominated aldehyde **8** (33% yield). Both compounds could be readily separated by silica gel column chromatography using a mixture of toluene/hexane (10/1) as eluent. The low yield of **7** might be due to steric hindrance caused by the styryl units in **5** during the cross-coupling reaction. Interestingly, the monobrominated and bis(styryl)-containing aldehyde **8** opens way to the synthesis of various types of bathochromically shifted conjugated dialdehydes as well as dibromo-derivatives, which can serve in further polycondensation reactions.

The resulting polymers from **7**, **DO-ST-PPE$_2$-PPV$_2$**, and **MEH-ST-PPE$_2$-PPV$_2$** were obtained as dark red substances in 58% and 96% yield, respectively, after allowing **7** to react with the corresponding bis(phosphonate ester) **9** based on a synthetic procedure described elsewhere.[15]

The chemical structures of **7**, **8**, and the polymers were confirmed by ^1H and ^{13}C NMR, IR and elemental analysis. The ^{13}C NMR spectrum (100 MHz, $CDCl_3$) of **7** is depicted in Figure 3, while Figure 4 shows the ^{13}C NMR spectrum (63 MHz, $CDCl_3$) of **MEH-ST-PPE$_2$-PPV$_2$**.

All the peaks can be readily assigned to the corresponding carbon atoms except in the region between 110 and 130 ppm, where an overlapping between aromatic and vinylene carbon peaks is observed, complicating an individual assignment to the respective carbon atoms.

The molecular weights of the polymers were determined by gel permeation chromatography using THF as eluent and polystyrene as standards. M_n and M_w values of 14 200 g/mol and 46 600 g/mol (PDI = 3.9) as well as 27 000 g/mol and 100 000 g/mol (PDI = 3.2) were estimated for **DO-ST-PPE$_2$-PPV$_2$** and **MEH-ST-PPE$_2$-PPV$_2$**, respectively. This results in degrees of polymerization of ∼11 and ∼21, respectively.

Thermogravimetry measurements carried out at a heating rate of 20 °C/min revealed an improvement of the thermal stability of approximately 30 °C after replacing dioctyloxy side groups with bis(styryl) units from **O-8-PPE$_2$-PPV$_2$** to **DO-ST-PPE$_2$-PPV$_2$**, and a decrease in the same range going from **DO-** to **MEH-ST-PPE$_2$-PPV$_2$**. 5% weight loss was recorded at 329 and 372 °C for **O-8-PPE$_2$-PPV$_2$** and **DO-ST-PPE$_2$-PPV$_2$**, respectively. The thermograms of the three **PPE$_2$-PPV$_2$** polymers are shown in Figure 5.

The photophysical properties of the compounds were investigated in dilute chloroform solution as well as in thin films in the case of the polymers. The solution absorption spectra, normalized fluorescence spectra and the fluorescence excitation anisotropy spectra of the starting materials **7**, **8**, and **10** as well as those of the polymeric materials are depicted in Figures 6

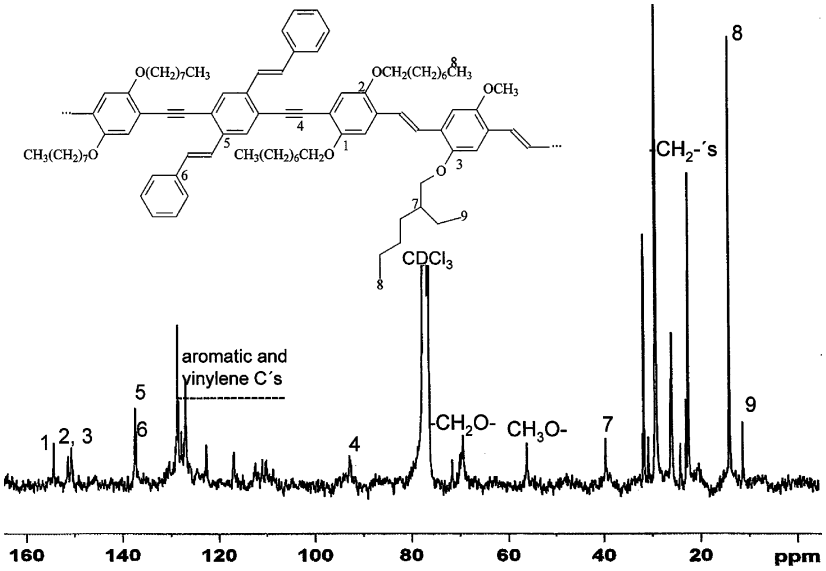

Figure 4. ^{13}C NMR spectrum ($CDCl_3$, 63 MHz) of **MEH-ST-PPE$_2$-PPV$_2$**.

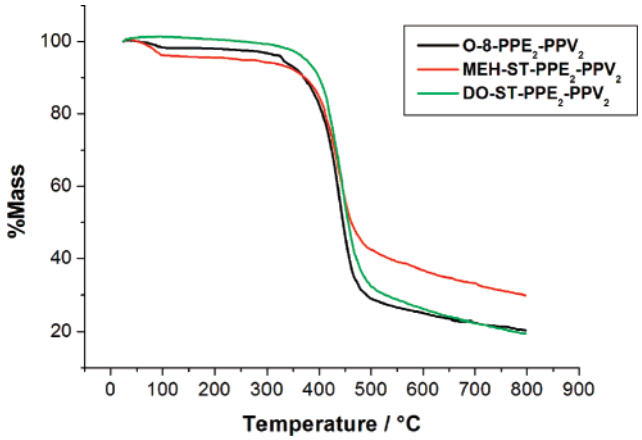

Figure 5. Thermogravimetry curves of the three **PPE$_2$-PPV$_2$** polymers. The heating rate was 20 °C/min under nitrogen.

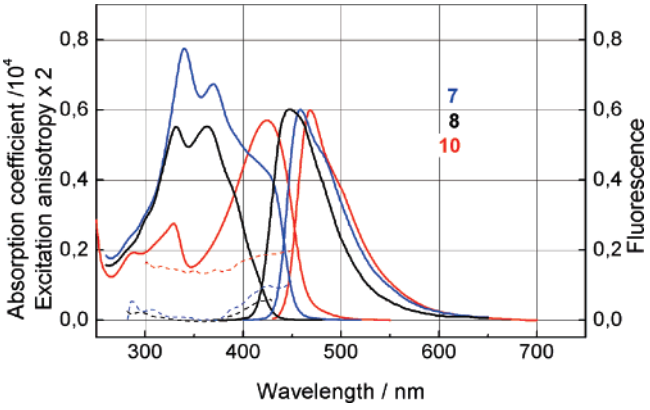

Figure 6. Absorption spectra (absorption coefficient divided by 10^4 M^{-1} cm^{-1}), normalized quantum corrected fluorescence spectra and fluorescence excitation anisotropy spectra (dashed line, multiplied by the factor 2) of compounds **7**, **8**, and **10** in $CHCl_3$ solution at room temperature.

and 7, respectively. The corresponding photophysical data are summarized in Table 1.

The absorption spectra of dialdehydes **7** and **10** clearly demonstrate the influence of the styryl-substitution. It obviously shortens the conjugation along the main chromophore system (OHC−Ph−C≡C−Ph−C≡C−Ph−CHO) compared to the alkoxy-substitution. This is reflected by a hypsochromic shift

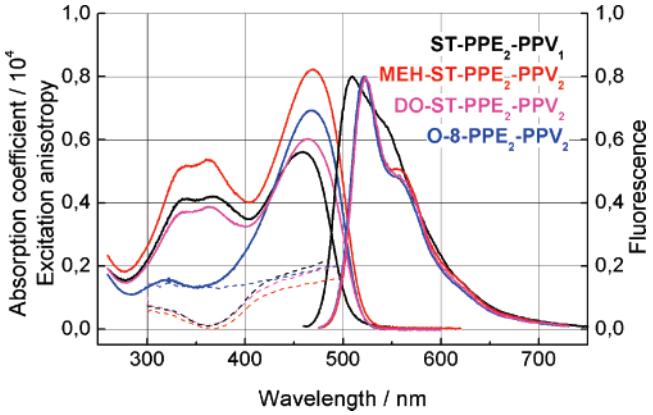

Figure 7. Absorption spectra (absorption coefficient per repeating unit divided by 10^4 M^{-1} cm^{-1}), normalized quantum corrected fluorescence spectra and fluorescence excitation anisotropy spectra (dashed line) of polymers in $CHCl_3$ solution at room temperature.

of the longest wavelength absorption edge and of the fluorescence spectrum as well as the reduction of the absorption coefficient around 425 nm. This blue shift can be ascribed to a twist of the main chromophore system resulting from steric hindrances generated by the styryl substituents. The actual $S_0 \rightarrow S_1$ ($\pi \rightarrow \pi^*$) electronic transition, located along the main axis, appears as a shoulder (425 nm) due to an overlapping with the absorption of the bis(styryl)phenylene chromophore system (Ph−CH═CH−Ph−CH═CH−Ph) around 360 nm. This assignment arises from the comparison of the fluorescence rate constants according to Strickler and Berg, k_f(SB),[17] calculated for different assumptions concerning the shape of $S_0 \rightarrow S_1$ absorption band with the corresponding absorption coefficients (Table 1), with the fluorescence rate constant k_f obtained from the ratio between the fluorescence quantum yield, Φ_f, and the fluorescence lifetime, τ ($k_f = \Phi_f/\tau$). The calculated k_f(SB) values, assuming the absorption peaks either around 340 or 369 nm to be $S_0 \rightarrow S_1$ electronic transition, are definitely too high compared to $k_f = \Phi_f/\tau$. Similar explanation can be made with compound **8**, despite its shorter chromophore system. Its $S_0 \rightarrow S_1$ electronic transition is also located in the low energy absorption edge around 400 nm. Compound **8** exhibits lower fluorescence quantum yield and shorter lifetime than **7** and **10**, resulting from enhanced radiationless deactivation due to the presence of bromine.

Table 1. Data from Absorption and Emission in Dilute Chloroform Solution

compound	λ_a/nm[a]	ϵ^a	E_g^{opt}/eV	λ_f/nm	Φ_f/%	r^b	τ/ns	k_f/ns^{-1} [c]	k_{nr}/ns^{-1} [d]	k_f(SB)/ns^{-1} [e]	k_f/k_f(SB)
	340	77 600	2.73	458	54	0.048	2.60	0.21	0.18	1.27	0.17
7	369	67 600								0.52	0.40
	425 sh	42 700								0.098	2.1
	332	55 300	2.89	447	11	0.029	0.74	0.15	1.20	0.98	0.15
8	363	55 000								0.47	0.32
	390 sh	35 000								0.070	2.1
10	424	57 000	2.61	468	65	0.095	1.44	0.45	0.24	0.51	0.88
O-8-PPE$_2$-PPV$_2$	469	69 300	2.36	521	60	0.18	0.74	0.81	0.54	0.51	1.6
ST-PPE$_2$-PPV$_1$	461	56 200	2.40	509	76	0.19	0.73	1.04	0.33	0.35	3.0
DO-ST-PPE$_2$-PPV$_2$	467	75 700	2.38	523	58	0.18	0.79	0.73	0.53	0.48	1.5
MEH-ST-PPE$_2$-PPV$_2$	471	82 300	2.38	522	49	0.15	0.77	0.64	0.66	0.51	1.3

[a] Monomers (**7**, **8**, **10**): absorption maxima or shoulders (sh) and their absorption coefficients. Polymers: longest wavelength absorption maxima and their absorption coefficients, taken per repeating unit. [b] Emission anisotropy at λ_f excited at the longest wavelength absorption maximum or at the shoulder (compounds **7** and **8**), calculated with $r = (I_{||} - GI_{\perp})/(I_{||} + G2I_{\perp})$. [c] $k_f = \Phi_f/\tau$: rate constant of the fluorescence transition [d] $k_{nr} = (1 - \Phi_f)/\tau$: sum of the rate constants of the nonradiative transitions [e] k_f(SB): rate constant of the fluorescence transition according Strickler/Berg.[17]

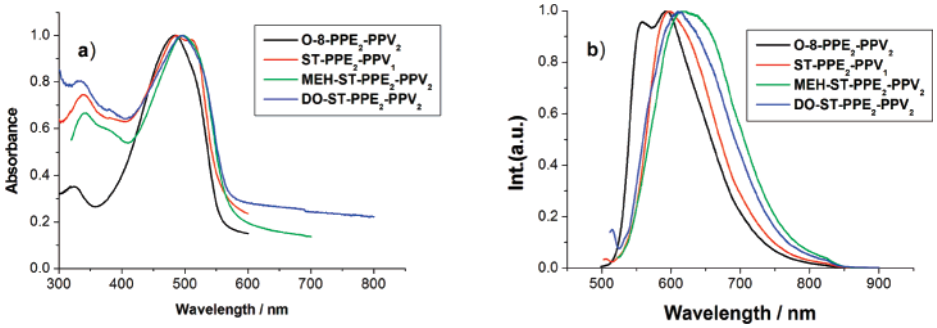

Figure 8. Normalized thin film absorption (a) and emission (b) spectra of the polymers. Films were spin-casted from a chlorobenzene solution.

Compared to the monomers, the absorption spectra of the polymers are characterized by bathochromically shifted intense and unstructured bands around 460−470 nm, due to extended chromophore system along the polymeric backbone. **ST-PPE$_2$-PPV$_1$** (461 nm) is slightly blue-shifted compared to the **PPE$_2$-PPV$_2$** polymers (λ_a = 467−470 nm) due to a smaller number of double bonds within its repeating unit (RU). Analogous to the monomers, the absorption bands in the shorter wavelength region around 360 nm in **ST-PPE$_2$-PPV$_1$**, **DO-ST-PPE$_2$-PPV$_2$**, and **MEH-ST-PPE$_2$-PPV$_2$** can be assigned to the bis(styryl)-phenylene chromophore system (Ph−CH═CH−Ph−CH═CH−Ph). This assignment is even more evident in the case of the polymers than of the monomers **7** and **8** through the course of the fluorescence excitation anisotropy spectra (Figures 6 and 7). Contrary to the solely alkoxy-substituted compounds, the emission anisotropy of the styryl-substituted compounds diminishes and reaches the value 0 around 360 nm, corresponding to the bis(styryl) system. On the basis of this value 0, the angle α between the transition moments of the absorption ($S_0 \rightarrow S_2$-transition) and the fluorescence ($S_1 \rightarrow S_0$-transition) can be estimated to be 55° using the well-known Perrin equation, eq 1:[18]

$$r = \frac{1}{5}(3\cos^2\alpha - 1) \qquad (1)$$

55° corresponds approximately to the angle of 60° expected between the polymer main chain and bis(styryl)phenylene chromophore system.

No significant influence of the styryl-substituents on the fluorescence spectra, fluorescence quantum yields and fluorescence lifetimes is observed when comparing polymers **O-8-PPE$_2$-PPV$_2$** with **DO-ST-PPE$_2$-PPV$_2$** and **MEH-ST-PPE$_2$-PPV$_2$**, all exhibiting a 2:2 of *triple bond*/*double bond* ratio. Their well-structured emission spectra consist of a $S_{10} \rightarrow S_{00}$ transition at ∼520 nm and a $S_{10} \rightarrow S_{01}$ transition at ∼ 560 nm. On the basis of the ratio between the fluorescence rate constants, $k_f = \Phi_f/\tau$ and k_f(SB), the effective fluorophore system is assumed consisting of one to two repeating units.[5b] The lower full-width-at half-maximum, fwhm$_f$ values (∼2300 cm^{-1}), compared to the monomers (2500−3000 cm^{-1}) and the strong structuring of the emission spectra, are indications of reduced flexibility at the excited state, as expected from higher molecular weight compounds.

Table 2. Data from Polymer Thin Film Absorption and Emission Spectra (Films Were Spin Cast from Chlorobenzene Solution)

compound	λ_a/nm	E_g^{opt}/eV	λ_f/nm	$FWHM_f$/cm^{-1}	Φ_f/%
O-8-PPE$_2$-PPV$_2$	484	2.24	559, *593*	3360	23
ST-PPE$_2$-PPV$_1$	487, 510	2.19	596	2830	14
DO-ST-PPE$_2$-PPV$_2$	499, 340, 384	2.14	610	3400	24
MEH-ST-PPE$_2$-PPV$_2$	497 *343, 370*	2.12	620	3400	9

The differences encountered in the emissive behavior of **ST-PPE$_2$-PPV$_1$** (approximately 12 nm blue-shifted and less structured emission spectrum as well as higher Φ_f and fwhm$_f$) are related to the 2:1 *triple bond*/*double bond* ratio.

Figure 8 depicts the thin film absorption and emission spectra of the four polymers. Thin films of approximately 100 nm were obtained after spin-coating from a chlorobenzene solution and drying in an oven for 8 h at 70 °C. Thin film photophysical data are given in Table 2. As expected, there is a bathochromic shift going from the solution to the thin film. This might be due to chromophore−chromophore interaction. Approximately 15 nm red shift of absorption and 40 nm of emission were obtained for the solely alkoxy-substituted polymer **O-8-PPE$_2$-PPV$_2$.** Twice as higher values were obtained for the styryl-substituted polymers, namely an approximately 30 nm red shift of absorption and 90 nm of emission. Similar to the solution, the thin film main absorption band of all the polymers is unstructured, except in the case of **ST-PPE$_2$-PPV$_1$,** which consists of two peaks at 487 and 510 nm; this might suggest

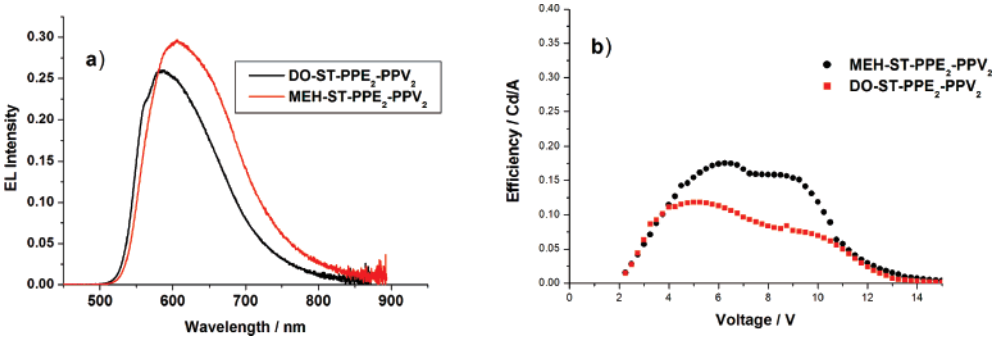

Figure 9. EL spectra (a) and efficiency-voltage characteristics (b) of both **ST-PPE$_2$-PPV$_2$** polymers. LED setup was as follows: glass substrate/ITO/PEDOT:PSS/**ST-PPE$_2$-PPV$_2$**/Ca/Ag.

various contributions of **H-** and **J**-aggregates.[19] The stronger electron-donating effect of the styryl-substitutents than alkoxy-substituents is reflected by an approximately 15 nm red shift of the main absorption band of the **ST-PPE$_2$-PPV$_2$** compounds (λ_a = 497−499 nm, E_g^{opt} = 2.12−2.14 eV) relative to **O-8-PPE$_2$-PPV$_2$** (λ_a = 484 nm, E_g^{opt} = 2.24 eV). The effect of the bis(styryl)phenylene chromophore system is moreover visible through the strong absorption in the UV-region between 300 and 400 nm. In contrast to the solution behavior, the bis(styryl)-phenylene peak around 380 nm is less intense than the peak around 340 nm assigned to the presence of alkoxy side chains. The strong hyperchromic effect of the 340 nm peak in the case of the styryl-substituted polymers **ST-PPE$_2$-PPV$_1$** and **ST-PPE$_2$-PPV$_2$** relative to the solely alkoxy-substituted polymer **O-8-PPE$_2$-PPV$_2$** might be an indication of *intensity borrowing* from the bis(styryl)phenylene peak.

The thin film emission spectrum of **O-8-PPE$_2$-PPV$_2$** consists of two peaks at 559 nm ($S_{10} \rightarrow S_{00}$) and 593 nm ($S_{10} \rightarrow S_{01}$) of nearly identical intensity. A Stokes shift of ca. 65 nm was obtained. In contrast totally unstructured thin film fluorescence spectra resulted from the styryl-substituted polymers; Stokes shifts of more than 100 nm were obtained in this case, suggesting strong backbone conformational differences between ground and excited states in addition to emission from aggregations and excimer-like species. Contributions from excimer-like species would explain the low Φ_f and the larger fwhm$_f$ values (>3000 cm^{-1}) compared to the solution. The slight red shift of the PL spectrum of **MEH-ST-PPE$_2$-PPV$_2$** (620 nm) and lower Φ_f relative to **DO-ST-PPE$_2$-PPV$_2$** (610 nm) is attributable to enhanced $\pi-\pi$ interchain interactions caused by the grafting of the short methoxy side groups. The same trend is observed in the EL spectra of both polymers recorded from LED-devices of the setup glass substrate/ITO/PEDOT:PSS/**ST-PPE$_2$-PPV$_2$**/Ca/Ag, as shown in Figure 9a. A red shift of ∼20 nm was obtained going from **DO-ST-PPE$_2$-PPV$_2$** (λ_{EL} = 584 nm, yellow) to **MEH-ST-PPE$_2$-PPV$_2$** (λ_{EL} = 605 nm, orange). Figure 9b displays the efficiency-voltage characteristics. Higher maximum luminous efficiency was obtained for **MEH-ST-PPE$_2$-PPV$_2$** (0.18 Cd/A at 6V) than for **DO-ST-PPE$_2$-PPV$_2$** (0.12 Cd/A at 5V). Very low turn on voltages around 2 V were recorded for both polymers. The slightly better LED performance of **MEH-ST-PPE$_2$-PPV$_2$** despite its lower Φ_f might be attributable to better $\pi-\pi$ interchain interactions and enhanced planarization, resulting in improved *inter*- as well as *intra*molecular recombination of the electrically generated holes (positive polarons) and electrons (negative polarons).[5e] A higher contribution of the efficiency of the recombination of injected charges, γ, to the overall electroluminescence efficiency, η_{EL}, is thus possible, knowing that η_{EL} is proportional to $\Phi_f \times \gamma$.[20]

The charge carrier extraction by linearly increasing voltage (CELIV) technique has been used to measure the mobility of

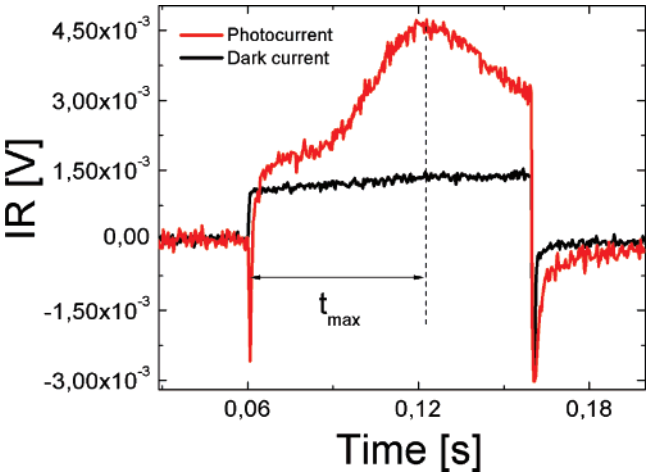

Figure 10. Charge carrier extraction by linearly increasing voltage (CELIV) current transients in **DO-ST-PPE$_2$-PPV$_2$**: Black bottom transient is the dark capacitive response to the applied triangle-shaped voltage pulse, whereas the red top transient demonstrates extraction of photogenerated charge carriers. The charge carrier mobility in the volume of the film is estimated from the extraction maximum time t_{max}.

the photogenerated charge carriers.[20] The idea of this technique is that after a laser pulse the photogenerated charge carriers are extracted inside the film with the applied triangle-shaped voltage pulse. The charge carrier mobility is then calculated directly from the current transient maximum position.[21]

The CELIV technique has the advantage over other electrical techniques that films of a broad range of conductivities can be studied, and that the carrier mobility is measured directly from the extraction time maximum in the current transient. The only restriction imposed by the experimental setup (the same as it is in the time-of-flight technique) is that at least one contact of the sample should be blocking (partially); otherwise, injection current would overlap and hinder the current transients.

The very initial current step $j(0)$ (displacement current) is caused by the geometrical capacity of the sample and can be used for estimation of the sample thickness or dielectric permittivity of the film when the sample thickness is known. The following increasing extraction current is caused by the photoconductivity of the sample due to the photogenerated charge carriers. As the triangle voltage pulse continues to increase, the electric field redistribution takes place inside the sample and carrier mobility values μ are calculated directly from the current transients:

$$\mu = \frac{2d^2}{At_{max}^2}$$

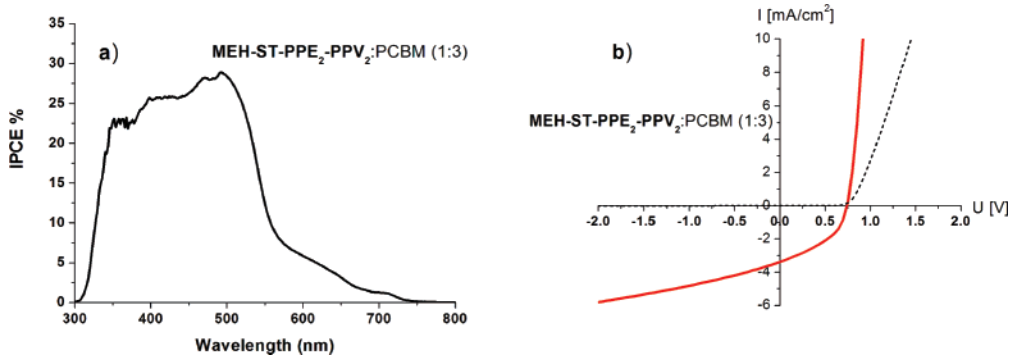

Figure 11. (a) Incident photon to current efficiency (IPCE) curve. (b) Current−voltage ($I-V$) curves of solar cell in dark (dashed line) and under illumination (solid line) with white light at irradiation of 100 mW/cm^2. Device configuration: glass substrate/ITO/PEDOT:PSS/**MEH-ST-PPE$_2$-PPV$_2$**:PCBM (1:3)/LiF/Al.

where d is the sample thickness, A the voltage rising slope (highest voltage of the triangle pulse divided by the pulse duration), t_{max} is the extraction maximum. The coefficient 2 used in this equation is due to the surface carrier photogeneration with strongly absorbed laser light (also thick films were used in the experiment to ensure that the product of absorption coefficient and film thickness is much larger than 1).

In Figure 10, the typical CELIV current transients are shown in the dark (black lower transient) and using short laser light pulse (red top transient). The same current transients were recorded for all three **PPE$_2$-PPV$_2$** polymers. The hole mobility was directly estimated from the current transient responses using maximum extraction time t_{max}. It was found to be 1.5×10^{-6}, 2.8×10^{-6}, and 5.5×10^{-6} cm^2/V·s in **DO-ST-PPE$_2$-PPV$_2$**, **MEH-ST-PPE$_2$-PPV$_2$**, and **O-8-PPE$_2$-PPV$_2$**, respectively. The electric field at the extraction maximum was approximately 16 kV/cm.

The dark current response were very similar for all studied polymers, demonstrating that the film conductivity is rather low (Maxwell's relaxation time $\tau_\sigma > 100$ ms), which is expected from clean, high quality undoped materials, where the equilibrium charge carrier concentration is low.

The charge carrier mobility was measured directly from the current transient response after the laser pulse (top red transient). The delay between laser and triangle voltage pulse was 1 μs and the laser pulse can be seen as a negative spike (at around 0.06 s) in the top red current transient. Since there were no significant dark injection even in forward bias using standard ITO and aluminum electrodes, it was possible to test the mobility of both electrons and holes. However, due to the very low electron mobility (at least 10 times less than hole mobility) in all studied polymers, it was impossible to experimentally determine the exact value, but it can be concluded that the electron mobility is much lower than the hole mobility.

The lower mobility values for the styryl-substituted polymers with respect to their solely alkoxy-substituted counterpart is related to the twist of their conjugated backbones caused by the styryl units. The **MEH-ST-PPE$_2$-PPV$_2$** hole mobility value is approximately twice as high as that of **DO-ST-PPE$_2$-PPV$_2$**, attributable to enhanced $\pi-\pi$ interchain interactions due to the grafting methoxy side chains.

Using **MEH-ST-PPE$_2$-PPV$_2$** as donor component in conjunction with $PC_{61}BM$ as acceptor in a nonoptimized bulk heterojunction solar cell of configuration: glass substrate/ITO/PEDOT:PSS/**MEH-ST-PPE$_2$-PPV$_2$**:PCBM (1:3 wt ratio)/LiF/Al resulted in a maximum *incident photon to current efficiency* (IPCE) of 28% (Figure 11a). The solar cell (area 12 mm^2), whose $I-V$ curve is depicted in Figure 11b, shows following photovoltaic characteristics: open circuit voltage, $V_{OC} = 750$ mV, short circuit current, $I_{SC} = 3.38$ mA, filling factor, FF = 41.5%, and energy conversion efficiency at air mass 1.5, $\eta_{AM1.5} = 1.05\%$.

Conclusion

Two PPE-PPV polymeric systems, denoted **DO-ST-PPE$_2$-PPV$_2$** and **MEH-ST-PPE$_2$-PPV$_2$**, bearing styryl side groups have been synthesized and characterized. Detailed and extensive photophysical studies on the polymers and their luminophoric starting materials **7** and **8** have been carried out. For comparison reason, the solely alkoxy-substituted polymer **O-8-PPE$_2$-PPV$_2$** and its monomer **10** as well as **ST-PPE$_2$-PPV$_1$** were also investigated. The effects of the styryl units are 2-fold: On the one hand, they act as electron donor (i.e., higher donor effect than alkoxy side groups) to the main chain conjugation; on the other hand, they form an independent *bis*styrylphenylene chromophore system, whose angle to the main chain has been estimated to be 55 °. The existence of two independent chromophore systems in **ST-PPE-PPV** systems was proven through the combination of absorption spectra and fluorescence excitation anisotropy spectra. Strong *intensity borrowing effects* were observed in the UV region of the absorption spectra between 300 and 400 nm. Red-shifted thin film PL and EL spectra together with improved EL performance were observed for **MEH-ST-PPE$_2$-PPV$_2$** as compared to **DO-ST-PPE$_2$-PPV$_2$**, as a result of stronger $\pi-\pi$ interchain interactions. The twist of the conjugated backone of **ST-PPE$_2$-PPV$_2$** polymers caused by the styryl side groups might be at the source of their lower intrinsic hole mobility values compared with the solely alkoxy-substituted counterpart **O-8-PPE$_2$-PPV$_2$**. Nevertheless, nonoptimized bulk heterojunction solar cells of $\eta_{AM1.5}$ around 1% were readily designed using **MEH-ST-PPE$_2$-PPV$_2$** as donor and PCBM as acceptor in a 1:3 weight ratio.

Acknowledgment. We are grateful to the group of Prof. Klaus Meerholz, Universität zu Köln, Cologne, Germany, for carrying out the electroluminescent studies, and to the Dutch Polymer Institute, the Fonds für Chemische Industrie, and NWO for financial support.

References and Notes

(1) (a) Brizius, G.; Pschirer, G. N.; Steffen, W.; Stitzer, K.; zur Loye, H.-C.; Bunz, U. H. F. *J. Am. Chem. Soc.* **2000**, *122*, 12435. (b) Bunz, U. H. F. *Acc. Chem. Rev.* **2001**, *34*, 998.

(2) (a) Egbe, D. A. M.; Tillmann, H.; Birckner, E.; Klemm, E. *Macromol. Chem. Phys.* **2001**, *202*, 2712. (b) Egbe, D. A. M.; Roll, C. P.; Birckner, E.; Grummt, U.-W.; Stockmann, R.; Klemm, E. *Macromolecules* **2002**, *35*, 3825.

(3) (a) Ramos, A. M.; Rispens, M. T.; van Duren, J. K. J.; Hummelen, J. C.; Janssen, R. A. J. *J. Am. Soc.* **2001**, *123*, 6714. (b) Schenning, A. P. H. J.; Tsipis, A. C.; Meskers, S. C. J.; Beljonne, D.; Meijer, E. W.; Brédas, J. L. *Chem. Mater.* **2002**, *14*, 1362.
(4) (a) Chu, Q.; Pang, Y.; Ding, L.; Karasz, F. E. *Macromolecules* **2003**, *26*, 3848. (b) Tong, M.; Sheng, C. X.; Yang, C.; Vardeny, Z. V.; Pang, Y. *Phys. Rev. B* **2004**, *69*, 155211.
(5) (a) Egbe, D. A. M.; Bader, C.; Klemm, E.; Ding, L.; Karasz, F. E.; Grummt, U.-W.; Birckner, E. *Macromolecules* **2003**, *36*, 9303. (b) Egbe, D. A. M.; Carbonnier, B.; Ding, L.; Mühlbacher, D.; Birckner, E.; Pakula, T.; Karasz, F. E.; Grummt. U.-W. *Macromolecules* **2004**, *37*, 7451. (c) Egbe, D. A. M.; Carbonnier, B.; Paul, E. L.; Mühlbacher, D.; Kietzke, T.; Birckner, E.; Neher, D.; Grummt, U.-W.; Pakula, T. *Macromolecules* **2005**, *38*, 6269. (d) Egbe, D. A. M.; Kietzke, T.; Carbonnier, B.; Mühlbacher, D.; Hörhold, H.-H.; Neher, D.; Pakula, T. *Macromolecules* **2004**, *37*, 8863. (e) Egbe, D. A. M.; Ulbricht, C.; Orgis, T.; Carbonnier, B.; Kietzke, T.; Peip, M.; Metzner, M.; Gericke, M.; Birckner, E.; Pakula, T.; Neher, D.; Grummt, U.-W. *Chem. Mater.* **2005**, *17*, 6022.
(6) (a) Ding, L.; Egbe, D. A. M.; Karasz, F. E. *Macromolecules* **2004**, *37*, 6124. (b) Ding, L.; Lu, Z.; Egbe, D. A. M.; Karasz, F. E. *Macromolecules* **2004**, *37*, 10031.
(7) Egbe, D. A. M.; Stockmann, R.; Hotzel, M. *J. Opt. A.: Pure Appl. Opt.* **2004**, *6*, 791.
(8) (a) Hoppe, H.; Egbe, D. A. M.; Mühlbacher, D.; Sariciftci, N. S. *J. Mater. Chem.* **2004**, *14*, 3462. (b) Al-Ibrahim, M.; Konkin, A.; Roth, H.-K.; Egbe, D. A. M.; Klemm, E.; Zhokhavets, U.; Gobsch, G.; Sensfuss, S. *Thin Solid Films* **2005**, *474*, 201. (c) Konkin, A.; Sensfuss, S.; Roth, H.-K.; Nazmutdinova, G.; Schroedner, M.; Al-Ibrahim, M.; Egbe, D. A. M. *Synth. Met.* **2005**, *148*, 199.
(9) (a) Egbe, D. A. M.; Nguyen, L. H.; Hoppe, H.; Mühlbacher, D.; Sariciftci, N. S. *Macromol. Rapid Commun.* **2005**, *26*, 1389. (b) Egbe, D. A. M.; Nguyen, L. H.; Hoppe, H.; Schmidtke, K.; Sariciftci, N. S. *J. Thin Solid Films* **2006**, *486*, 511−512. (c). Kietzke, T.; Shin, R. Y. C.; Egbe, D. A. M.; Chen, Z.-K.; Sellinger, A. *Macromolecules* **2007**, *40*, 4424.
(10) Kietzke, T.; Egbe, D. A. M.; Hörhold, H.-H.; Neher, D. *Macromolecules* **2006**, *39*, 4018.
(11) Wilson, J. N.; Windscheif, P. M.; Evans, U.; Myrick, M. L.; Bunz, U. H. F. *Macromolecules* **2002**, *35*, 8681.
(12) Demas, J. N.; Crosby, G. A. *J. Phys. Chem.* **1971**, *75*, 991.
(13) Blum, J.; Zimmerman, M. *Tetrahedron* **1972**, *28*, 275.
(14) Egbe, D. A. M.; Bader, C.; Nowotny, J.; Günther, W.; Klemm, E. *Macromolecules* **2003**, *36*, 5459.
(15) Egbe, D. A. M.; Nguyen, L. H.; Schmidtke, K.; Wild, A.; Guenes, S.; Sieber, C.; Sariciftci, N. S. *J. Polym. Sci., Part. A: Polym. Chem.* **2007**, *45*, 1619.
(16) (a) Tohda, Y.; Sonogashira, K.; Hagihara, N. *Synthesis* **1977**, 77. (b) Bunz, U. H. F. *Chem. Rev.* **2000**, *100*, 1605.
(17) Strickler, S. J.; Berg, R. A. *J. Chem. Phys.* **1962**, *37*, 814.
(18) (a) Perrin, F. *Ann. Phys.* **1929**, *12*, 169. (b) Kawski, A. *Crit. Rev. Anal. Chem.* **1993**, *23*, 459.
(19) (a) Bouchard, J.; Belletête, M.; Durocher, G.; Leclerc, M. *Macromolecules* **2003**, *36*, 4624. (b) Moliton, A.; Nunzi, J.-M. *Polym. Int.* **2006**, *55*, 583.
(20) Moliton, A.; Hiorns, R. C. *Polym. Int.* **2004**, *53*, 1397.
(21) Juska, G.; Arlauskas, K.; Viliunas, M.; Kocka, J. *Phys. Rev. Lett.* **2000**, *84*, 4946.

MA071676I